International Journal of Medical, Medicine and Health Sciences
ISSN: 2517-9969
Vol:7, No:6, 2013

Development of a Brain Glutamate Microbiosensor

Kartika S. Hamdan, Zainiharyati M. Zain, Mohamed I. A. Halim, Jafri M. Abdullah, and Robert D. O'Neill

***Abstract*—**This work attempts to improve the permselectivity of poly-*ortho*-phenylenediamine (PPD) coating for glutamate biosensor applications on Pt microelectrode, using constant potential amperometry and cyclic voltammetry. Percentage permeability of the modified PPD microelectrode was carried out towards hydrogen peroxide (H_2O_2) and ascorbic acid (AA) whereas permselectivity represents the percentage interference by AA in H_2O_2 detection. The 50-µm diameter Pt disk microelectrode showed a good permeability value toward H_2O_2 (95%) and selectivity against AA (0.01%) compared to other sizes of electrode studied here. The electrode was further modified with glutamate oxidase (GluOx) that was immobilized and cross linked with glutaraldehyde (GA, 0.125%), resulting in Pt/PPD/GluOx-GA electrode design. The maximum current density J_{max} and apparent Michaelis constant, K_M, obtained on Pt/PPD/GluOx-GA electrodes were 48 µA cm^{-2} and 50 µM, respectively. The linear region slope (LRS) was 0.96 µA cm^{-2} mM^{-1}. The detection limit (LOD) for glutamate was 3.0 ± 0.6 µM. This study shows a promising glutamate microbiosensor for brain glutamate detection.

***Keywords*—**Brain, Glutamate, Microbiosensor.

I. Introduction

GLUTAMATE (Glu) is an important neurotransmitter in the mammalian brain. The neurotransmitter plays a main role in development of brain, neurotransmission, synaptic plasticity, neurotoxicity and is involved in neurological disorders: ischemia [1], [2] schizophrenia [3], epilepsy [4], [5], Alzheimer's disease (AD) [6], [7], and Parkinson's disease (PD) [8]. A motivation for a better understanding about the function of glutamate as a neurotransmitter in brain it is crucial for the observation of extracellular glutamate levels released from neurons and glial cells [9].

Recent discoveries have revealed that glutamatergic neurotransmission in the central nervous system (CNS) is mediated by a dynamic interaction between neurons and astrocytes which is most abundance of glutamate level in hippocampus where the glutamate receptor is the major excitatory receptor [10], [11], [31]. There are several methods applied for brain glutamate detection such as magnetic resonance [6], capillary electrophoresis [12], [13], high performance liquid chromatography (HPLC) [14] and on-line microdialysis [15], [16]**.** The interest of electroanalytical neuroscientists in brain glutamate detection using modified electrodes is due to their advantage in term of high sensitivity and selectivity, reproducibility, low cost, and fast and accurate results. Biosensors are particularly helpful in the understanding of brain neurotransmitter physiology especially in vivo [17]-[19]. A key design criterion for implantation of in-vivo biosensors is the need to minimize the size without compromising H_2O_2 permeability and AA selectivity and sensitivity, thus reducing brain tissues damage. In this study, we focused on comparing different electrode sizes and several electrode architectures.

K. S. Hamdan, Z. M. Zain, and M. I. A. Halim are with the Faculty of Applied Sciences, Universiti Teknologi MARA (UiTM), 40450 Shah Alam, Selangor, Malaysia (corresponding email: zainihar@salam.uitm.edu.my).

J. M. Abdullah is with the Department of Neuroscience, School of Medical Sciences, Health Campus, Universiti Sains Malaysia (USM), 16150 Kubang Kerian, Kelantan, Malaysia.

R. D. O'Neill is with the UCD School of Chemistry & Chemical Biology, University College Dublin, Belfield, Dublin 4, Ireland (corresponding email: Robert.ONeill@UCD.ie).

II. Materials and Methods

L-Glutamate (Glu), glutamate oxidase from *Streptomyces sp*. (GluOx), glutaraldehyde (GA), *o*-phenylenediamine (*o*-PD), L-ascorbic acid (AA), and H_2O_2 (30% w/w, aqueous solution) were obtained from Sigma Aldrich, without further purification. The background electrolyte used for both PPD electropolymerization and calibration before and after PPD modification was a phosphate-buffered saline (PBS). PBS buffer was prepared of 300 mM, pH 7.46 consisting of NaCl (Merck, 150 mM), NaOH (Sigma, 40 mM) and NaH_2PO_4 (Sigma, 40 mM). All solutions were freshly prepared on the day the experiments were carried out.

A. Fabrication of Working Electrode

The platinum–iridium (Pt-Ir) (90:10) working electrodes used throughout this study were fabricated using stress relieved Teflon® insulated wire, of internal diameter 125 µm (5T), 25 µm and pure platinum (99.99) of internal diameter 50 µm. Pt electrodes were prepared from 4 cm length of Teflon coated wire. At one end of the wire, approximately 3 mm of Teflon was stripped away using scalpel to expose the bare wire and was soldered into gold connectors. The other end of the electrode was cut again to get a fresh cut disk. The bare Pt electrodes were then modified using various methods.

B. Electropolymerization: Poly (o-Phenylenediamine) (PPD) Preparation

In this study PPD was coated on top of Pt wire using either amperometric or cyclic voltammetry (CV) scan technique. A fresh PBS stock (pH 7.46) was prepared to produce 300 mM of *o*-PD. A 25 ml of stock solution of *o*-PD was prepared by dissolving 0.811 g approximately in a 25 ml volumetric flask with nitrogen (N_2) saturated PBS with the aid of a sonicator until it dissolved. Electropolymerization of *o*-PD in amperometric technique was carried out at a constant potential of +700 mV vs. Ag/AgCl for 30 min. Electropolymerization with CV was carried out by scanning the potential from 0 to +700 mV with scan rate 20 mV s^{-1} over 60 cycles [24]. The modified electrode is abbreviated as Pt/PPD.

C. Enzyme Immobilization

Pt/PPD was dipped in the GluOx solution (200 U ml^{-1}) which was diluted in 1.0 ml of distilled water in an Eppendorf tube five times (~0.5 s); electrodes were air dried for 5 min between each dip. The number of GluOx dips on Pt/PPD/GluOx was investigated in this work.

D. Glutaraldehyde (GA, 1%)

After GluOx immobilization on Pt/PPD, electrodes were then dipped in 1% GA by dipping the electrodes (~0.5 s) once and air dried for 5 min to produce Pt/PPD/GluOx-GA. Effects of GA concentration on Pt/PPD/GluOx-GA were studied.

E. Instrumentation and Software

Electropolymerizations and calibrations were performed in a standard three-electrode electrochemical cell. An Ag/AgCl with 3 M KCl was used as reference electrode and a stainless steel needle served as an auxiliary electrode. Constant potential amperometry was performed at +700 mV applied potential using Autolab (Netherland) controlled by software 1.7 NOVA. +700 mV vs. Ag/AgCl with a scan rate of 20 mV s^{-1} over 60 cycles. Meanwhile, the different modification of Pt electrodes served as the working electrode.

F. Amperometric calibrations

All hydrogen peroxide (H_2O_2) and ascorbic acid (AA) calibrations were performed in 20 ml PBS using amperometry. After a stable current was achieved approximately after 45 min, aliquots of AA interference were administered and followed by administration of Glu (10, 20, 40, 100, 200 µL giving a final concentration of 1 mM). H_2O_2 calibrations ranged from 0 to 0.1 mM and AA calibrations in the range 0–1 mM were performed on all electrodes before and after modification in nitrogen saturated PBS. All experiments were carried out at room temperature. The sensitivity of the various coated electrodes was determined by calculating the slope of the analyte calibration curve by linear regression analysis. Selectivity value was calculated as a ratio of sensitivity of each interfering species to H_2O_2 sensitivity on a molar basis. The steady-state AA calibration at Pt/PPD is distinctively non-linear, forming a flat plateau of response. This non-linear calibration has been interpreted in terms of self-blocking by AA or its oxidation products, trapped in the polymer matrix [20]. The values are reported are mean of current density ± standard deviation (SD) with *n* being the number of sensors.

III. Results and Discussion

An important approach in recent biosensor development is modification of the electrode so that it is suitable for implantation in brain tissue, especially for glutamate monitoring. In this investigation, electrode diameters determine the area of tissue damage caused by the insertion of the probe. The implantable biosensor must be able to reject electrochemical species by incorporation of a permselective membrane coating on the surface of the electrode, such as electropolymerization of PPD [21], [22] which also facilitates enzyme immobilization [23].

A. H_2O_2 and AA Calibration on Bare Electrodes

The H_2O_2 sensitivity of a series of different diameters of disk electrode is compared in Table I. The sensitivity of bare Pt towards H_2O_2 and AA was calculated according to previously reported work [24], [25].

TABLE I
Sensitivity of Pt Bare Electrodes towards H_2O_2 and AA

Pt bare electrode diameter *n*=3	Sensitivity (µA cm^{-2} mM^{-1}) ± SD	
	H_2O_2	AA
125 µm (Pt_{125})	181 ± 11	188 ± 48
50 µm (Pt_{50})	319 ± 16	207 ± 56
25 µm (Pt_{25})	732 ± 110	342 ± 16

The sensitivity of electrodes towards H_2O_2 and AA for different diameters of bare Pt disk. Mean of current density (µA cm^{-2} mM^{-1}) ± standard deviation (SD).

As exhibited in Table I, Pt_{25} bare electrodes have the highest current density with correlation coefficient, R^2= 0.998 followed by Pt_{50}, R^2= 0.999 and Pt_{125} with the lowest sensitivity, yet still having a high value of R^2= 0.998. Thus there was a difference in signal response between the three different sizes of diameter, although they gave a linear plot in the range of concentration 0–0.1mM. Meanwhile the calibration for AA, Pt_{25} also showed the highest slope of current density compared to other sizes of electrode. There was no significant difference between H_2O_2 and AA slopes for Pt_{125} and Pt_{50}. Therefore, Pt_{25} could be the most suitable for the development of biosensors since it is a smaller size among the other electrodes and gave a better performance in terms of measuring H_2O_2 and AA.

B. H_2O_2 and AA Calibration on Pt/PPD Electrodes

Among the advantages of Pt/PPD in biosensor design are the high permeability to the oxidase transduction molecule H_2O_2 [23] and its ultra-thin dimension on the electrode surface that enables enzyme immobilization adequately without any reaction activity [22]. In addition, for in vivo neurochemical monitoring, the PPD membrane is stable over a period of continuous measurement [26]. Furthermore, the ability of PPD to reject AA is an important property that enables the detection of neurochemicals in vivo [27]-[29].

We observed that bare Pt_{25} showed a better measured H_2O_2 and AA sensitivity. However, after the electropolymerization of PPD on the electrode surface, Pt_{50}/PPD (302 ± 28µA cm^{-2} mM^{-1}, R^2= 0.999) showed a higher current for calibration of H_2O_2, followed by Pt_{125}/PPD (180 ± 27µA cm^{-2} mM^{-1}, R^2= 0.999).

The response in AA calibrations for PPD modified electrodes formed a flat plateau (graph not shown). Both Pt_{50}/PPD (1.7 ± 0.7µA cm^{-2} for 1mM) and Pt_{125}/PPD (1.2 ± 3.6 µA cm^{-2} for 1mM) showed a small difference in value. This indicated that the PPD layer deposited on the electrode surface acted as barrier to AA which is an interference species in brain extracellular fluid (ECF). Thus, H_2O_2 gave a higher response compared to AA in terms of current density for Pt/PPD. Meanwhile, Pt_{25}/PPD showed a high current density of AA

measurement (32 ± 41μA cm^{-2} mM^{-1}, R^2= 0.998). Therefore, they still had the ability to reject interference species but less so. We considered that Pt_{25}/PPD has poorer ability to block AA compared to other sizes of electrode; the PPD layer formed on the electrode surface was enough to reduce sensitivity of AA [20]. This has been summarized in Fig. 1. Based on the research from McMahon et al [20], there could be different kinetics of deposition of the PPD membrane onto different sizes of Pt electrode.

C. Permeability and Selectivity of Pt/PPD Electrode

The oxidation current was recorded for AA and H_2O_2 at constant potential, under the same experimental conditions for all sizes of Pt/PPD electrodes. Based on Table II data, Pt_{125}/PPD showed a high permeability of H_2O_2 and the other hand, at Pt_{25}/PPD H_2O_2 was not detected. Nevertheless, Pt_{125} offers a low permeability for AA to diffuse to the electrode surface. This shows the rejecting properties of permselective membrane has given good results. Though, technically, Pt_{25}/PPD can provide better rejection of AA [17], [30] in this context shows a different opinion. From this value, we considered that Pt_{25}/PPD unable to repel an electroactive species by PPD membrane layer because of the possibility from Teflon holes enable AA species to migrate to the electrode surface. Also the possibility of formation PPD layer on Pt_{125}/PPD and Pt_{25}/PPD have produced a high peak current which form a thick layer of PPD membrane compared to Pt_{50}/PPD from the result of Table III.

Given the conclusion from Fig. 1, percentage selectivity parameters for Pt/PPD electrodes for different sizes in diameter were analyzed. Pt_{50}/PPD has a lower selectivity towards AA compared to Pt_{125}/PPD.

TABLE II
PERMEABILITY OF PT ELECTRODE

Pt/PPD (electrode diameter) *n* = 3	Analyte	% Permeability P% ± SD
125 μm	H_2O_2	100 ± 3
	AA	0.63 ± 0.07
50 μm	H_2O_2	94 ± 2
	AA	0.8 ± 0.1
25 μm	H_2O_2	ND
	AA	9.4 ± 2.6

Permeability, P%= slope (H_2O_2) or (AA) at Pt/PPD divided by slope (H_2O_2) or (AA) at bare Pt times 100. Permeability of Pt electrode for all different sizes of diameter after polymerized by *o*-PD. ND= not detected for the calibration of H_2O_2 for Pt_{25}/PPD.

D.Microbiosensor Performance of Pt_{50}/PPD/GluOx-GA Electrode

The reaction between GluOx and glutamate with oxygen as electron acceptor as follows:

$$\text{L-Glutamate} + H_2O_2 + \text{GluOx/FAD} \rightarrow \alpha\text{-ketoglutarate} + NH_3 + \text{GluOx/FADH}_2 \quad (1)$$

$$\text{GluOx/FADH}_2 + O_2 \rightarrow \text{GluOx/FAD} + H_2O_2 \quad (2)$$

$$H_2O_2 \rightarrow O_2 + 2H^+ + 2e^- \quad (3)$$

TABLE III
PEAK CURRENT OF ELECTROPOLYMERIZATION

Pt/PPD (electrode diameter), *n* = 3	Current Density (μA cm^{-2} mM^{-1}) ± SD
125 μm	271545 ± 5
50 μm	2034 ± 5
25 μm	49400 ± 2

Peak current of electropolymerization of *o*-PD using CV by scanning the potential from 0 to +700 mV vs. Ag/AgCl with scan rate 20 mV s^{-1} for different sizes of electrode.

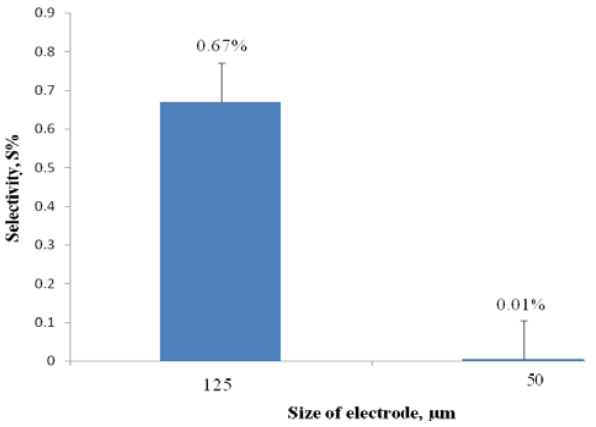

Fig. 1 Selectivity, S%= Current of AA (1mM) at Pt/PPD divided by current density of H_2O_2 (slope) at Pt/PPD times 100, determination for two different size of Pt/PPD electrode, *n* = 3

A biosensor is usually designed to operate in real applications within the linear region of analyte response. The excellent rejection of AA by Pt_{50}/PPD/GluOx-GA using different concentration of GA is detected, where the most suitable concentration was 0.125%. The cross-linked GA helps the immobilization of GluOx become stronger to be attached onto the surface electrode. The narrow cross sectional area 1.96 x $10^{-5}$$cm^2$ make this biosensor the promising electrode for implantable biosensor for brain Glu detection which is give a stronger electrode compared to Pt_{25} that very delicate and easily bent. Also, the size of Pt_{50} is smaller than Pt_{125} that give the opportunity for development of microbiosensor to reduce tissue damage. Pt_{50}/PPD/GluOx-GA biosensor, incorporating the enzyme GluOx and GA after electropolymerized by PPD for increase the sensitivity of electrode. Later, the modified electrode was calibrated for Glu in vitro. The calibration result for Glu is shown in Fig 2. The sensitivity of Glu in the linear range of the Michaelis-Menten calibration curve was 70 ± 9 μA cm^{-2} mM^{-1}, *n* = 3, R^2= 0.944 with linear region slope (LRS) 0.96μA cm^{-2} mM^{-1}. The maximum of current density, J_{max} and apparent Michaelis constant, K_M were 48μA cm^{-2} and 50μM, respectively. The limit of detection (LOD) for Pt_{50}/PPD/GluOx-GA in Glu detection was 3.0 ± 0.6μM.

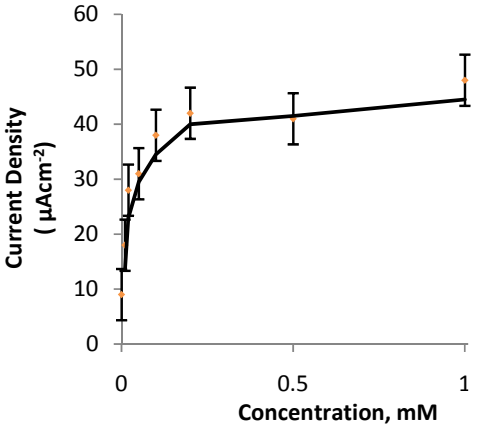

Fig. 2 The Glu response at Pt_{50}/PPD/GluOx-GA (0.125% GA) biosensor, showing the Michaelis-Menten calibration curve. The J_{max}=48 µA $cm^{-2}$and K_M=50 µM were obtained

IV. Conclusion

The purpose of this work was to develop a glutamate biosensor; Pt_{50}/PPD/GluOx-GA was chosen because of its low permeability and high selectivity against AA, the main interference species in brain analysis. This rejection of electroactive interference was due to the electropolymerized PPD which formed an ultra-thin layer with good sensitivity to both exogenous and enzyme-generated H_2O_2.

Acknowledgments

This work is supported by FRGS grant (600-RMI/ST/FRGS 5/3/Fst (12/2011) and MyMaster (MyBrain15) Scheme to Kartika S. Hamdan awarded from Ministry of Higher Education (MOHE), Malaysia.

References

[1] S. Baltan, "Ischemic injury to white matter: an age-dependent process," *Neuroscientist*, 15(2), 2009, pp. 126-33.
[2] A. Camacho, and L. Massieu, "Role of glutamate transporters in the clearance and release of glutamate during ischemia and its relation to neuronal death," *Archives of medical research,* 37(1), 2006, pp. 11-8.
[3] C. R. Breese, R. Freedman, S. S. Leonard, "Research report: Glutamate receptor subtype expression in human postmortem brain tissue from schizophrenics and alcohol abusers," *Brain Research*, 674, 1995, pp. 82-90.
[4] T. L. Babb, Z. Ying, J. Hadam, and C. Penrod, "Glutamate receptor mechanisms in human epileptic dysplastic cortex," *Epilepsy Research*, 32, 1998, pp. 24-33.
[5] S. C. Buckingham, and S. Robel, "Glutamate and tumor-associated epilepsy: Glial cell dysfunction in the peritumoral environment," *Neurochemistry International*, 2013.
[6] N. Fayed, P. J. Modrego, and G. Rojas-Salinas, and K. Aguilar, "Brain Glutamate Levels Are Decreased in Alzheimer's Disease : A Magnetic Resonance Spectroscopy Study," *American Journal of Alzheimer's Disease and Other Dementias*, 26 (6), 2011, pp. 450-456.
[7] Y. Gong, C. F. Lippa, J. Zhu, Q. Lin, and A. L. Rosso, "Disruption of glutamate receptors at Shank-postsynaptic platform in Alzheimer's disease," *Brain Research*, 1292, 2009, pp. 191-298.
[8] A. W. Amara, R. L. Watts, , and H. C. Walker, "The effects of deep brain stimulation on sleep in Parkinson's disease," *Therapeutic Advances in Neurological Disorders*, 4(1), 2011, pp. 15-24.
[9] T. S. Rao, K. D. Lariosa-Willingham, and N. Yu, "Glutamate-dependent glutamine, aspartate and serine release from rat cortical glial cell cultures," *Brain Research*, 978, 2003, pp. 213-222.
[10] N. Kang, J. Xu, Q. Xu, M. Nedergaard, and J. Kang, "Astrocytic Glutamate Release-Induced Transient Depolarization and Epileptiform Discharges in Hippocampal CA1 Pyramidal Neurons," *J. Neurophysiol,* 94, 2005, pp. 4121-4130.
[11] B. Benz, G. Grima, and K. Q. Do, "Glutamate-induced homocysteic acid release from astrocytes: Possible implication in glia-neuron signalling," *Neuroscience*, 124, 2004, pp. 377–386.
[12] W. H. Church, C. S. Lee, and K. M. Dranchak, "Capillary electrophoresis of glutamate and aspartate in rat brain dialysate: Improvements in detection and analysis time using cyclodextrins," *Journal of Chromatography B*, 700, 1997, pp. 67-7.
[13] S. Tucci, C. Pinto J. Goyo, P. Rada, and L. Hernandez, "Measurement of Glutamine and Glutamate by Capillary Electrophoresis and Laser Induced Fluorescence Detection in Cerebrospinal Fluid of Meningitis Sick Children," *Clinical Biochemistry*, 31(3), 1998, pp. 143-150.
[14] F. Xu, M. Gao, L. Wang, and L. Jin, "Study on the effect of electromagnetic impulse on neurotransmitter metabolism in nerve cells by high-performance liquid chromatography–electrochemical detection coupled with microdialysis," *Analytical Biochemistry*, 307, 2002, pp. 33-39.
[15] S. Tucci, P. Rada, M. J. Sepulveda, and L. Hernandez, "Glutamate measured by 6-s resolution brain microdialysis: Capillary electrophoretic and laser-induced fluorescence detection application," *Journal of Chromatography B*, 694, 1997, pp. 343-349.
[16] Y. Yu, Q. Sun, T. Zhou, M. Zhu, L. Jin, and G. Shi, "On-line microdialysis system with poly(amidoamine)-encapsulated Pt nanoparticles biosensor for glutamate sensing in vivo," *Bioelectrochemistry*, 81, 2011, pp. 53-5.
[17] N. Wahono, P. Qin, P. Oomen, T. I. F. Cremers, M. G. de Vries, and B. H. C. Westerink, "Evaluation of permselective membranes for optimization of intracerebral amperometric glutamate biosensors," *Biosensors and Bioelectronics*, 33(1), 2012, pp. 260-266.
[18] M. G. Garguilo, and A. C. Michael, "Amperometric microsensors for monitoring choline in the extracellular fluid of brain," *Journal of Neuroscience Methods*, 70(1), 1996, pp. 73-82.
[19] J. P. Lowry, M. Miele, R. D. O'Neill, M. G. Boutelle, and M. Fillenz, "An amperometric glucose-oxidase/poly(*o*-phenylenediamine) biosensor for monitoring brain extracellular glucose: in vivo characterisation in the striatum of freely-moving rats," *Journal of Neuroscience Methods*, 79, 1998, pp. 65-74.
[20] C. P. McMahon, S. J. Killoran, S. M. Kirwan, and R. D. O'Neill, "The selectivity of electrosynthesised polymer membranes depends on the electrode dimensions: implications for biosensor applications," *Chem Comm*, 2004, pp. 2128-2130.
[21] N. Hamdi, J. Wang, and H. G. Monbouquette, "Polymer films as permselective coatings for H_2O_2-sensing electrodes," J*ournal of Electroanalytical Chemistry*, 581, 2005, pp. 258-264.
[22] S. Myler, S. Eaton, and S. P. J. Higson, "Poly (*o*-Phenylenediamine) ultra thin polymer-film composite membranes for enzyme electrodes," *Analytica Chimica Acta*, 357, 1997,pp. 55-61.
[23] J. D. Craig, and R. D. O'Neill, "Electrosynthesis and permselective characterisation of phenol-based polymers for biosensor applications," *Analytica Chimica Acta*, 495, 2003, pp. 33-43.
[24] S. A. Rothwell, C. P. McMahon, and R. D. O'Neill, "Effects of polymerization potential on the permselectivity of poly(*o*-phenylenediamine) coatings deposited on Pt–Ir electrodes for biosensor applications," *Electrochimica Acta*, 55, 2010, pp. 1051-1060.
[25] C. P. McMahon, G. Rocchita, S. M. Kirwan, S. J. Killoran, P. A. Serra, J. P. Lowry, and R. D. O'Neill, "Oxygen tolerance of an implantable polymer/enzyme composite glutamate biosensor displaying polycation-enhanced substrate sensitivity," *Biosensors and Bioelectronics*, 22, 2007, pp. 1466-1473.
[26] S. J. Killoran, and R. D. O'Neill, "Characterization of permselective coatings electrosynthesized on Pt–Ir from the three phenylenediamine isomers for biosensor applications," *Electrochimica Acta*, 53, 2008, pp. 7303-7312.
[27] B. M. Dixon, J. P. Lowry, R. D. O'Neill, "Characterization in vitro and in vivo of the oxygen dependence of an enzyme/polymer biosensor for monitoring brain glucose," *Journal of Neuroscience Methods*, 119, 2002, pp. 135-142.

[28] J. C. Vidal, E. Garcia, and J. R. Castillo, "In situ preparation of overoxidized PPyroPPD bilayer biosensors for the determination of glucose and cholesterol in serum," *Sensors and Actuators B*, 57, 1999, pp. 219-226.
[29] Z. M. Zain, R. D. O'Neill, J. P. Lowry, K. W. Pierce, M. Tricklebank, A. Dewa, and S. A. Ghani, "Development of an implantable D-serine biosensor for in vivo monitoring using mammalian D-amino acid oxidase on a poly (*o*-phenylenediamine) and Nafion-modified platinum–iridium disk electrode," *Biosensors and Bioelectronics*, 25, 2010, pp. 1454-1459.
[30] K. B. O'Brien, S. J. Killoran, R. D. O'Neill, and J. P. Lowry, "Development and characterization in vitro of a catalase-based biosensor for hydrogen peroxide monitoring," *Biosensors and Bioelectronics,* 22 (12), 2007, pp. 2994-3000.
[31] M. C. Angulo, A. S. Kozlov, S. Charpak and E. Audinat, "Glutamate released from glial cells synchronizes neuronal activity in the hippocampus," *The Journal of Neuroscience*, 24 (31), 2004, pp. 6920-6927.